Penetration and Mixing of Multiple Gas Jets Subjected to a Cross Flow

LEONARD S. COHEN,* LAWRENCE J. COULTER,† AND WILLIAM J. EGAN JR.‡
United Aircraft Research Laboratories, East Hartford, Conn.

An experimental study of the interaction of a high-velocity airstream with jets from single row, multihole wall injectors is presented. Results are reported for tests conducted at nominal airstream Mach numbers of 0.6, 2, and 3. Injectant fluids included helium, argon, and Freon-12. One supersonic and twelve sonic wall injectors having various hole spacings, hole diameters, and injection angles were employed in these tests. The influence of a disturbed approach flow boundary layer on jet penetration and mixing was determined in tests with blowing upstream of the injector. Schlieren photographs of the injectant flowfield were taken and Pitot pressure, total temperature, and species concentration profiles were obtained at several tunnel locations. These data were employed to develop correlations for the penetration height, the distance required to achieve two-dimensional flow, and the kinematic eddy viscosity. The latter correlation establishes a connection between downstream mixing and initial jet penetration. It was found that small amounts of blowing upstream of the injectors significantly increases jet penetration and the rate of subsequent jet-airstream mixing.

Nomenclature

a = local tunnel height, cm
b = tunnel width, cm
C = local concentration, kg/kg-total
C_D = drag coefficient
C_{f_0} = local friction factor—no blowing
D = injector circular hole exit flow diameter, which includes discharge coefficient correction, cm
D^* = injector hole throat diameter, cm
FAR = fuel-to-air ratio
H = penetration height, cm
H_{MID} = penetration height taken as the distance from the wall to the center of Mach disk, cm
H_{TOP} = penetration height taken as the distance from the wall to the top of the Mach disk, cm
k,k_1,k_2 = constants in various equations
L = characteristic blockage length, see Fig. 10, cm
M = Mach number
N = characteristic blockage dimension, cm
n = power law exponent
P = pressure, atm
P_{eb} = effective back pressure for jets discharging into a supersonic cross flow, atm
P^* = pressure at nozzle throat, atm
S = injector plate hole spacing measured between hole centerlines, cm
V = velocity, m/sec
v_b = transverse blowing velocity, m/sec
W = weight flow, kg/sec
X = longitudinal distance from injector holes, cm
Z = vertical distance measured from tunnel floor, cm
Z^* = Gaussian half-width location, cm
$\bar{Z}$ = centroid of fuel profile defined in Eq. (2), cm
α = angle of injection measured from mainstream flow direction, deg
γ = ratio of specific heats
δ = boundary-layer thickness, cm
δ^* = displacement thickness, cm
ϵ = eddy viscosity, kg/(m-sec)
θ = momentum thickness, cm
ρ = density, kg/m³

Subscripts

b = blowing
I = injectant
L = refers to lower portion of skewed Gaussian
M = values at the maximum of the Gaussian
$0,o$ = quantity evaluated at $X = 0$
P = Pitot
T = total conditions
THR = threshold conditions
U = refers to upper portion of skewed Gaussian
∞ = mainstream

Received June 25, 1970; revision received September 28, 1970. Work supported in part by AFAPL, Contract AF 33(615)-5153.

* Supervisor, Aerothermochemistry Group, Air-Breathing Propulsion Section. Member AIAA.
† Senior Research Engineer, Aerothermochemistry Group, Air-Breathing Propulsion Section. Member AIAA.
‡ Research Engineer, Aerothermochemistry Group, Air-Breathing Propulsion Section; presently at Florida Research and Development, United Aircraft Corporation. Member AIAA.

I. Introduction

A METHOD for predicting the fuel distribution downstream of a fuel injector is essential in the evolution of a viable design procedure for supersonic combustion ramjets, because combustor stability, heat release rate, and combustion efficiency all depend on local stoichiometry. Since the usual mode of introducing fuel into a scramjet combustor is via one or more rows of discrete ports flush-mounted in the combustor wall, the analytical model employed must treat the initial interaction of fuel jets with the mainstream air as well as the turbulent mixing of fuel and air downstream of the injection station. Furthermore, as a practical matter, the description of these processes should be expressed in terms of initial fuel and airflow conditions and physical properties, and injector characteristics.

Previous contributions to this problem[1-10] were largely confined to the description of initial fuel penetration and to the understanding of the impingement zone with its various shocks and separation regions in the vicinity of a single hole injector. Of particular note, was the demonstration by Spaid[1] of the existence of a characteristic length scale that may be obtained from schlieren photographs of the disturbed flowfield at the injector. Zukoski and Spaid[2] were later able to calculate this important length scale by assuming it was equal to the radius of a quarter sphere blunt body which produces a shock pattern similar to that resulting from jet injection. An alternative characteristic length measured from the combustor wall to the center of the Mach disk associated with the expanding fuel jets has been proposed by Schetz and Billig.[3]

Notwithstanding the body of existing work which relates to injectors discharging into high-speed airstreams, the available data were judged inadequate for the purpose of formulating a design procedure capable of predicting the fuel distribution in a scramjet combustor mixing region prior to ignition. A lack of data was noted relative to: 1) the mutual interactions that occur between jets from adjacent holes in a row; 2) the connection between downstream mixing and the interactions that occur initially between injectant streams and the main airflow; and 3) the influence of the approach flow boundary layer on jet penetration.

The work described herein was undertaken with the objectives of developing the needed data base for the construction of a semi-empirical combustor design procedure and ultimately verifying the predictions generated by any such procedure.

II. Description of the Flowfield

The flow pattern which results when gaseous fuel is introduced from an injector hole into a supersonic mainstream is shown in Fig. 1. The bow shock associated with the obstruction of the mainstream air caused by injection generally separates the wall boundary layer and gives rise to a complex flow similar to that found upstream of a forward facing step.[11] The underexpanded sonic jet shown here expands into the lower surrounding pressure and displays the characteristic Mach disk of jets entering a quiescent medium. Flow immediately downstream of the jet resembles that encountered for a back step.

Note that the injectant jet is turned as a result of its interaction with the mainstream flow so that the Mach disk is inclined to the horizontal. A jet penetration height may be selected as the distance from the wall to the top of the Mach disk, H_{TOP} (Ref. 6) or the distance from the wall to the center of the Mach disk, H_{MID}, following Schetz and Billig.[3] It will be shown that either one of these lengths is a useful scaling parameter for jet penetration.

Jets in a row mix with the airstream to ultimately eliminate all three-dimensional variations in the flow. Downstream, in the two-dimensional region, injectant concentration profiles may be fitted with skewed Gaussian distributions characterized by a maximum concentration, C_M, at $Z = Z_M$ and different half widths for the upper and lower portions of the distribution. That is,

$$(C/C_M)_I = \exp\{-0.693[(Z - Z_M)/(Z_j^* - Z_M)]^2\} \quad (1)$$

in which Z_j^* is either Z_U^* or Z_L^* the location of the half widths of the upper and lower portions of the profile. The parameters needed to describe the distributions of Eq. (1), are determined from fuel concentration measurements. Such data taken at various axial locations in the two-dimensional region may be extrapolated upstream to the injector location to define an effective two-dimensional source flow. In particular,

$$\bar{Z} = \left(\frac{b}{W_I}\right)\int_0^a C_I \rho V Z dZ \quad (2)$$

the centroids of the measured downstream fuel profiles can be used to find the effective centroid at $X = 0$, i.e., $\bar{Z} = \bar{Z}_0$,

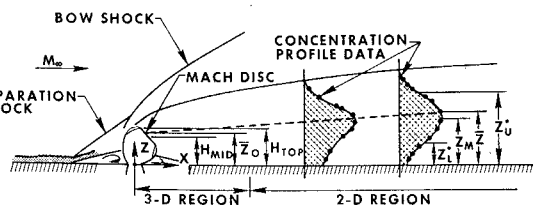

Fig. 1 Flowfield and nomenclature.

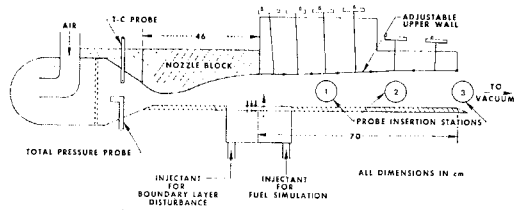

Fig. 2 Schematic diagram of tunnel test facility.

which turns out to be a useful length scale for the two-dimensional flowfield.

Within the two-dimensional region the fuel spreading rate may be evaluated using an appropriate kinematic eddy viscosity model. In the present work, an airstream is disturbed by blockages caused by injected wall jets in much the same manner as flow is disturbed when passing through screens. Thus by analogy to flow through screens, the jet-induced blockages may be expected to produce a high level of turbulence in the flow. Although the turbulence originating in this manner decays rapidly, it is far more significant than that produced by other available mechanisms and hence controls downstream mixing. This concept of an "aerodynamic screen" provides the connection between the injection/penetration process and downstream mixing of injectant and freestream air. An eddy viscosity formulation embodying this concept was derived in Ref. 12 using the initial period decay law found for isotropic turbulence downstream of grids. It has the form

$$\epsilon/\rho = kNV_\infty C_D \quad (3)$$

where N is a characteristic blockage dimension, $\frac{1}{2}\rho_\infty V_\infty^2 C_D$ is the drag of unit cross-sectional area of the blockage, and k is a proportionality constant determined from the detailed mixing data.

III. Experimental Study

Test Apparatus

The two-dimensional, continuous-flow wind tunnel used for the test work is shown in Fig. 2. The facility test section has an initial cross-sectional area of 10 cm × 10 cm and an adjustable upper wall along its usable length of 70 cm. Flow Mach numbers of approximately 0.6, 2, and 3 may be obtained by insertion of available nozzle blocks. The wind-tunnel floor contains numerous pressure taps and two (removable) plates. Helium, argon, and Freon-12 are injected through the downstream plate to simulate the injection of various fuels; small quantities of gas may also be introduced from the upstream plate to alter the approach flow boundary layer.

Air is delivered to the tunnel at flow rates up to 2.5-kg/sec from a 27-atm supply and is ultimately exhausted to atmosphere through vacuum pumps. Fuel is delivered at pressures up to 14-atm from a bottled gas supply system. Freon-12 is heated to a temperature of 320°K to ensure that this fluid is in gaseous form when injected.

The wall-mounted injector plates for the introduction of simulated fuel each contain a single row of equally spaced holes. The plenum side of the holes is counterbored for a 15° nozzle throat approach; the supersonic injector is also counterbored from the tunnel side giving an exit to throat area ratio of 1.531. Experimentally determined discharge coefficients ranging from 0.90 to 0.98, for the various injector plates, were applied as required in the data reduction. The thirteen different injector plates used provided the three hole diameters 0.0813, 0.132, and 0.260 cm, the three hole spacings, 0.412, 0.825, and 1.24 cm, injection angles in the range $60° \leq \alpha \leq 120°$ and injector area ratios of 1.0 and 1.531. Note that the supersonic injector is sized for injection of argon at a

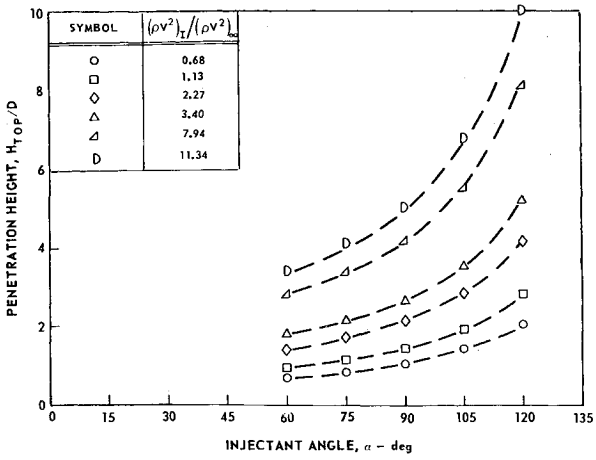

Fig. 3 Influence of injector angle on penetration.

Mach number of 2.0 (equivalent to the injection of Freon-12 at a Mach number of 1.78). The plate through which mass was injected to disturb the approach flow boundary layer contains 79, 0.45-cm-diam holes arranged in a random pattern. Blowing occurs over an axial length of 2.06 cm starting 5.4 cm upstream of the center-line through the row of fuel injector holes.

Probe Instrumentation

A five-probe rake and a thermocouple boundary-layer probe were employed to gather detailed local measurements throughout the tunnel. Either probe can be installed on a three-axis traversing mechanism which fits into access ports in the tunnel wall. Local Pitot pressures and species concentrations are measured with the rake which contains five probe tips made from 0.052-cm hypo-tubing. During operation with the rake, an automatic control system enables the five local pitot pressures to be recorded simultaneously. Then gas samples are obtained sequentially from each of the probes for analysis by an on-line, time-of-flight mass spectrometer. A complete cycle, including pressure and concentration measurements and purges for the five locations of the rake is completed in approximately 45 sec. The thermocouple boundary-layer probe is used when pressure and temperature measurements adjacent to the tunnel wall are required. The probe head opening is roughly a rectangle with a height and width of 0.025-cm and 0.075-cm, respectively. Other details of the probe designs are given in Ref. 13.

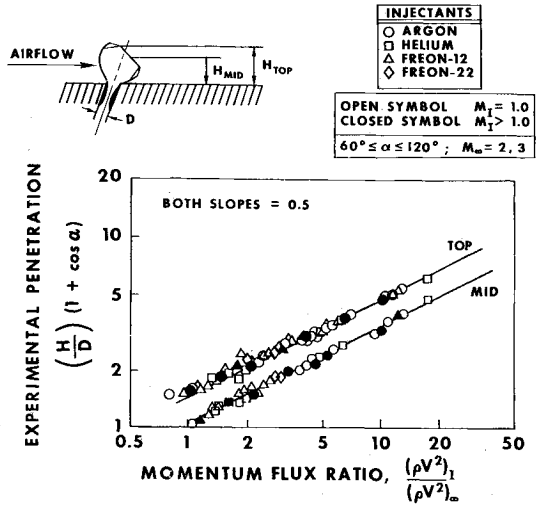

Fig. 4 Correlation of the penetration height.

Tunnel Calibration

Pitot pressure surveys were made at various axial and transverse locations to establish freestream and boundary-layer characteristics of the tunnel. The tunnel characteristics were also measured for a disturbed flow in which there was upstream wall injection (blowing) of air. Freestream Mach numbers of 0.55 ± 0.018, 1.90 ± 0.038, and 2.92 ± 0.044 were measured; Mach numbers of 0.6, 2, and 3, respectively, will be used for identification purposes throughout this paper. Examination of the experimental Mach number profiles and schlieren photographs revealed that the supersonic approach flows were shock-free. Mach number profiles at a given axial location 2 cm or more from a tunnel side wall were found to be indistinguishable from each other. Although findings of this nature are not sufficient to establish tunnel two-dimensionality, they nevertheless emphasize the regular, predictable nature of the approach flows in the center portion of the tunnel.

Boundary-layer measurements adjacent to the tunnel floor were fit with a power law profile to obtain the exponent n and the boundary-layer thickness δ for each approach flow. These results along with computed displacement and momentum thicknesses for the undisturbed boundary layers and the single disturbed boundary layer appear in Table 1.

Test Data

Data were gathered to provide information on the axial extent of the three-dimensional flow region downstream of the row of discrete fuel orifices, penetration heights from schlieren photographs, tunnel wall static pressures, plenum conditions, and detailed species concentration, Pitot pressure, and total temperature surveys. A complete tabulation of the data is contained in Ref. 14.

Concentration, Pitot pressure, and total temperature data were reduced to yield local species mass fractions, velocities, densities, and static temperatures. These results were subsequently employed in integrations of conservation equations to compute flow rates, over-all momentum, and over-all energy as checks on the dependability of the measurements. Data retained for analysis (comprising 98% of the total) yielded integrated fuel weight flows which were within ±5% of the venturi-measured (delivered) values. Comparisons of integrated momentum and energy with values calculated from initial airstream and injectant conditions were within ±10% for all data.

As a consequence of turbulent diffusion, discrete jets at the injection station gradually merge to lose their separate identities. The completion of this process, which marks the end of the region containing three-dimensional variations in flow properties and species concentrations, may be detected by measuring Pitot pressure and/or fuel concentration profiles in line with an injector hole and between adjacent holes at various axial locations. The axial distance at which no differences can be discerned between two such adjacent profiles is taken as the beginning of the two-dimensional flow re-

Table 1 Approach flow boundary-layer characteristics

	M_∞		
	0.6	2	3
n	10	7	5.3
δ, cm	3.40	0.91 (1.05)[a]	0.82
δ^*, cm	0.41	0.22 (0.28)	0.18
θ, cm	0.29	0.072 (0.12)	0.051

[a] Values in parentheses for disturbed approach flow boundary layer with blowing parameter ≅14.

gion. Correlations of these data (presented in Sec. IV) were frequently consulted to ensure that all profile data taken for this study were in the two-dimensional region.

IV. Experimental Results

Penetration Heights

Penetration heights associated with the top and mid point of injectant jet Mach disks were obtained from schlieren photographs of jet interactions with supersonic airstreams where the structure of the flow was easily discernable; photographs of jet interactions with subsonic air contained little detail and, therefore, were unsatisfactory for the establishment of penetration heights. Correlation of the penetration heights was achieved by using the injectant to freestream momentum flux ratio, and the injector angle factor $(1 + \cos\alpha)$. Adoption of the momentum flux ratio as the correlating group for penetration was indicated from a straightforward extension of the analytical results of Zukoski and Spaid.[2] The influence of injector angle on penetration was determined from the detailed data reproduced in Fig. 3. Figure 4 contains all the data with the recommended correlations for H_{MID} and H_{TOP}. Note that the two penetration heights yield parallel curves, reflecting an identical dependence on momentum flux ratio. Thus the two definitions of length scale are compatible and either one may be chosen for use. The equations of the curves in Fig. 4 are

$$\frac{H}{D} = \frac{k_1}{(1 + \cos\alpha)}\left[\frac{(\rho V^2)_I}{(\rho V^2)_\infty}\right]^{0.5}; \begin{cases} H = H_{\text{TOP}}, k_1 = 1.51 \\ H = H_{\text{MID}}, k_1 = 1.05 \end{cases} \quad (4)$$

The usefulness of the penetration height as a length scaling parameter was evident in the present work where it was found that the length of the upstream separation region normalized with the penetration height H_{MID} had a value of 4.14 ± 0.1.

The correlations of Eq. (4) are applied to pertinent data in Fig. 5 with satisfactory results. One additional correlation is also shown for H_{MID}: a relation proposed by Billig et al.,[7] which was evolved from data obtained by Crist et al.,[15] for sonic jets of various fluids discharging into quiescent air. Billig proposed that the penetration height, H_{MID}, be expressed as,

$$\frac{H_{\text{MID}}}{D_I^*} = \left[M_I^{1/2}\left(\frac{P_I^*}{P_{eb}}\right)\right]^{0.5} \quad (5)$$

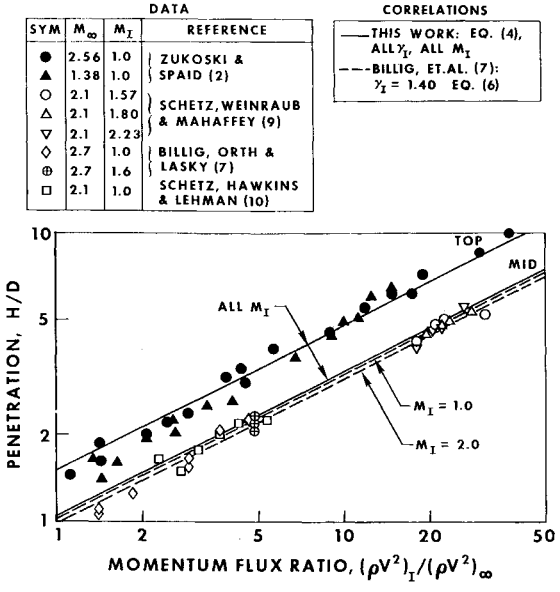

Fig. 5 Summary of available penetration data with correlations.

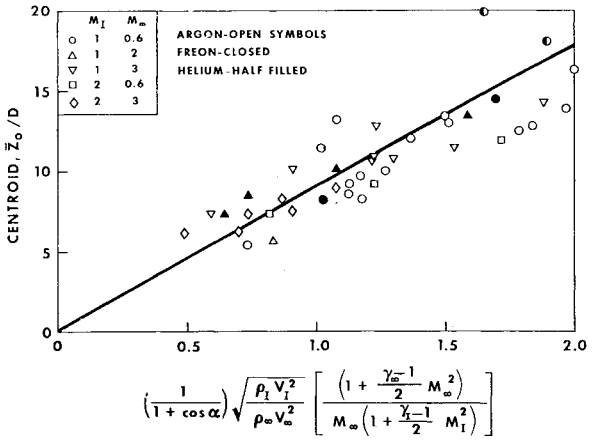

Fig. 6 Centroid correlation.

where P_{eb}, the effective back pressure, replaces P_∞ for expanding jets subjected to a cross flow. P_{eb} is taken equal to 80% of the static pressure behind a normal shock in the airstream.[10] Equation (5) may be cast in terms of the momentum flux ratio as required in Fig. 5 by introducing various compressible flow functions, with the result

$$\frac{H_{\text{MID}}}{D} = \left[\frac{2\left(1 + \frac{\gamma_I - 1}{2}M_I^2\right)}{\gamma_I^2 M_I(\gamma_I + 1)}\right]^{0.25} \times \left[\frac{1.25(1 + \gamma_\infty)\gamma_\infty M_\infty^2}{(1 - \gamma_\infty) + 2\gamma_\infty M_\infty^2}\right]^{0.5}\left[\frac{(\rho V^2)_I}{(\rho V^2)_\infty}\right]^{0.5} \quad (6)$$

The term involving γ_∞ and M_∞ is essentially a constant equal to $(1.5)^{0.5}$ for $M_\infty \geq 2.0$. However, note that variations with both the injectant Mach number and ratio of specific heats are indicated; for $\gamma_I = 1.10$, the factor multiplying the momentum flux ratio term is 1.17 for $M_I = 1.0$ and 1.015 for $M_I = 2.0$; for $\gamma_I = 1.667$, the comparable values are 0.948 and 0.843. Variations of this nature were not apparent in the present study.

Centroid of the Fuel Concentration Profiles

The penetration height, while acknowledged as a useful length scale parameter, is a property associated with the injection of a discrete jet and, therefore, with a three-dimensional flowfield. A search for a length scale which is more appropriate for a two-dimensional effective source flow led to the adoption of the (extrapolated) centroid of the fuel distribution profile at the injector station, $\bar{Z}_0$. This parameter was correlated for all of the flow conditions (subsonic and supersonic) and all of the injector geometries investigated as shown in Fig. 6. The slope of the correlating line drawn in the figure is 9.05.

Use of $\bar{Z}_0$ as a Correlating Parameter

Many of the important features of the injection and downstream mixing regions correlate with $\bar{Z}_o$. For example, the extent of the three-dimensional flow region downstream of injection as determined from pitot pressure data, depends on this parameter and hole spacing in the simple fashion displayed in Fig. 7. The expression $(X/S)(\bar{Z}_o/S) = 1$, a convenient representation of the pressure data, underscores the importance of hole spacing in determining the length required to mix out three-dimensional variations in the flow. For a given hole spacing, most rapid mixing (shortest three-dimensional region) is found for large values of $\bar{Z}_o$. Thus mixing is promoted in the initial region by increasing the fuel-to-air momentum flux ratio and/or the injection angle, at least over the range of angles investigated. Also shown in

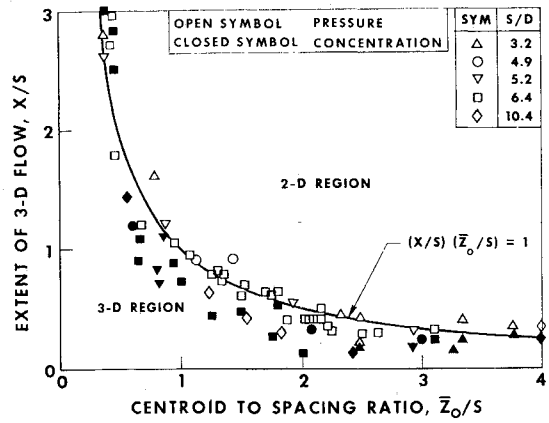

Fig. 7 Correlation for the two-dimensional flow boundary.

Fig. 7 are two-dimensional region boundaries determined from fuel concentration profile data. In general, three-dimensional variations in concentration are mixed out more rapidly than variations in pitot pressure.

It is of interest to have a description of the injectant concentration profile at the two-dimensional flow boundary. As demonstrated in Fig. 8, data taken close to the two-dimensional flow boundary may be described accurately using the Gaussian distribution of Eq. (1). In order to construct the Gaussian at the two-dimensional boundary for any conditions of interest the lengths Z_U^*, Z_M, and Z_L^*, and the maximum concentration are all required. The three lengths have been determined from extrapolations of corresponding lengths found for the measured downstream fuel concentration profiles. $\bar{Z}_o$ emerges again as a suitable correlating scale, as shown in Fig. 9. Note that the extrapolations were made to the injection location to yield $Z^*_{U,o}$, $Z_{M,o}$ and $Z^*_{L,o}$. These lengths are nearly identical to those which would be obtained at the two-dimensional flow boundary since the axial distances over which the extrapolations were made are at least an order of magnitude larger than the three-dimensional region lengths. The various correlations are given in Fig. 9. The maximum concentration, C_{M_o}, may be computed using Eq. (1) and these correlations in the conservation of fuel equation once information is available on the local mass flux distribution.

Kinematic Eddy Viscosity

Measured distributions of fuel concentration and velocity at the several axial locations along the tunnel were used to

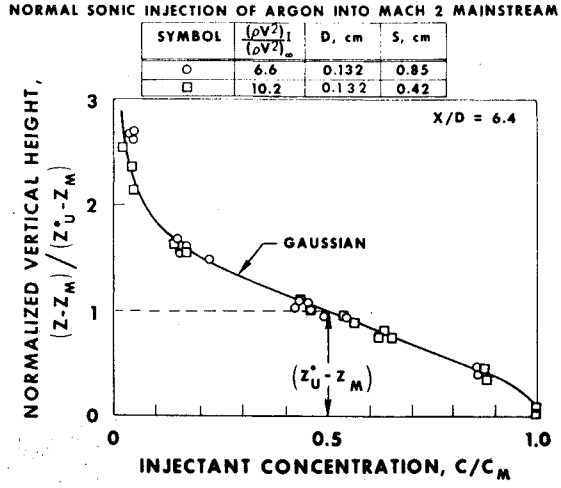

Fig. 8 Comparison of typical experimental profiles with Gaussian distribution.

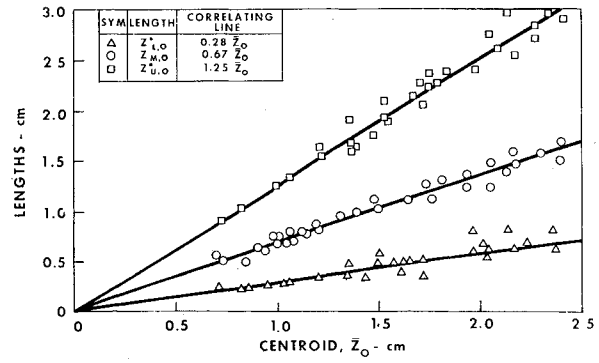

Fig. 9 Characteristic lengths determined from extrapolations to $X = 0$.

establish a value of the kinematic eddy viscosity which characterizes the mixing in the two-dimensional region for each combination of initial conditions and injector characteristics. Sets of profiles taken at an axial distance of 3.25 cm from the injection station served as the initial conditions for a computer solution of the boundary-layer equations. Application of such an analysis presumes that pressure varies in the longitudinal direction only. The inference from wall pressure measurements[2] is that this condition is satisfied beginning at a location $X \approx 4\ H_{TOP}$ downstream of the injection station. Thus in the present study the boundary-layer approximations can be expected to hold for $X/D > 20$. Trial computations were carried out with several different values of ϵ/ρ until predicted profiles at $X/D > 80$ were found to be in agreement with data. The values of ϵ/ρ determined in this manner reflect the influence of turbulence produced by jet blockage as well as the turbulence present initially in the freestream, designated $(\epsilon/\rho)_\infty$.

A confirmation of the aerodynamic screen model embodied in Eq. (3) to predict the kinematic eddy viscosity was sought and the results of this effort are summarized in Fig. 10. The freestream turbulence contribution, $(\epsilon/\rho)_\infty$, was fixed at a value which resulted in a zero intercept for the "best" straight line through the values of ϵ/ρ established from the data. At low values of injectant-to-air momentum flux ratio, disturbances created by the fuel injection are minimal so that downstream mixing is controlled by the level of turbulence initially present in the freestream. However, as the jet momentum flux is increased and additional blockage of the mainstream occurs, the turbulence produced as a result of flow interaction with the blockage elements exceeds the mainstream turbulence and ultimately dominates the fuel-air mixing process. If the combination of mainstream and injection conditions at which flow blockage begins to exert a measurable influence on downstream mixing rates are designated as the threshold (THR) conditions, then

$$\epsilon/\rho = (\epsilon/\rho)_\infty; \quad V_\infty L \leq (VL)_{THR} \tag{7}$$

$$\epsilon/\rho = (\epsilon/\rho)_\infty + 0.042\, C_D[V_\infty L - (VL)_{THR}]; \quad V_\infty L > (VL)_{THR} \tag{8}$$

in which L, as defined on Fig. 10, emerges as the characteristic blockage length; this parameter differs from the various penetration heights by a constant [see Eq. (4)]. $(VL)_{THR} = 0.465 M_\infty$ m²/sec is an empirical result that may depend on the characteristics of the flow system. Fortunately, exact specification of the threshold values is probably not critical since very rapid mixing is desirable for practical propulsion devices. The form of the drag coefficient adopted encompasses both supersonic and subsonic flows, although the transonic regime is specifically excluded. The drag coefficient was determined from the relation,

$$C_D = k_2 |M_\infty^2 - 1|^{-1/3} \tag{9}$$

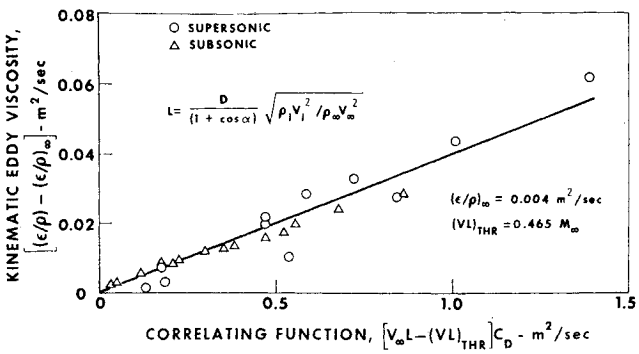

Fig. 10 Kinematic eddy viscosity correlation.

a form which was found to be useful by Werle,[16] in correlating pressure coefficients on jets injected from slots. The constant of proportionality k_2 is expected to be of order unity since a sphere and a spanwise cylinder have drag coefficients of 0.45 and 1.2, respectively, for low-speed flow at the Reynolds number of the Mach 0.6 tests. Accordingly, a unity value was used in the calculation for Fig. 10.

Fuel Distribution Design Procedure

The results described previously may be coordinated into an approximate, but useful procedure for predicting fuel distribution in the two-dimensional region of a duct into which fuel is injected from a single row of holes. Given the initial freestream and fuel conditions and the injector geometry, the extrapolated centroid is determined using Fig. 6. Then the two-dimensional flow boundary can be located using Fig. 7, and the kinematic eddy viscosity can be obtained from Fig. 10. Also, the fuel profile at the two-dimensional boundary can be generated provided the maximum fuel concentration is known. As noted earlier the determination of C_{M_o} requires information on the local mass flux profile. A useful approximation is to take $(\rho V)_o = (\rho V)_\infty$ (1 + FAR), where FAR is the over-all fuel air ratio. Then

$$C_{M_o} = W_I\left[b\int_0^a (\rho V)_o\left(\frac{C}{C_M}\right)dZ\right]^{-1} = 0.975\left(\frac{W_I/W_\infty}{1+\mathrm{FAR}}\right)\left(\frac{1}{\bar{Z}_o/a}\right) \quad (10)$$

All the required ingredients are available, therefore, for use in a solution of the boundary-layer equations to generate the downstream fuel distribution. It should be noted that mixing in the two-dimensional region is slow so that the profile constructed at the two-dimensional boundary might be profitably applied without resorting to boundary-layer computations in decisions concerning placement of downstream fuel injectors and pilots, and duct contouring.

Influence of Disturbing the Approach Flow Boundary Layer

In order to investigate the effect on penetration and fuel distribution of the characteristics of the approach flow boundary layer, small quantities of various gases were introduced into the tunnel from a multihole wall injector upstream of and adjacent to the fuel injector plate during some of the supersonic tests. This transpiration of material into the mainstream air thickened and generally disturbed the boundary layer approaching the injection station. The effect of this material addition on the freestream was minimal for values of the blowing parameter $\rho_b v_b/[\rho_\infty V_\infty(C_{f_o}/2)]$ less than 20, as no waves could be detected in schlieren photographs of the flow in these tests.

The use of upstream blowing to disturb the approach flow boundary layer was found to result in profound changes in jet

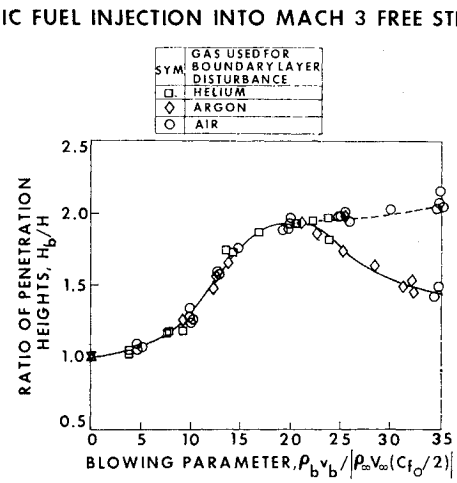

Fig. 11 Effect of upsteam blowing on penetration.

penetration and downstream mixing. As depicted in Fig. 11, a factor of two increase in penetration height was achieved for a blowing parameter value of 20; this corresponds to a blowing to freestream weight flow ratio of 0.0026. Presentation of the data in terms of the blowing parameter and the normalized penetration height is seen to eliminate any dependencies on the properties of the transpired fluid. Thus any fluid may be used to produce the desired increase in penetration; the use of fuel for this purpose might be particularly convenient. For blowing parameters greater than about 20, there is a falling off in the penetration height ratio. The dashed curve indicated in Fig. 11 is observed during unstable flow conditions and should not be used for design purposes.

A comparison of mixing profile measurements from comparable tests at $M_\infty = 2$ with a disturbed boundary layer and a normal boundary-layer (see Table 1) also reveals remarkable differences. The data in Fig. 12 reflects the augmented mixing rate and improved fuel coverage obtained with upstream blowing. The blowing parameter was about 14 for these tests. It is interesting to note that downstream mixing is enhanced to the degree which would be predicted by utilizing a value of L multiplied by the normalized penetration from Fig. 11 to find an ϵ/ρ from Fig. 10.

The transpiration process is known to effect significant changes in boundary-layer structure. In particular, a blown boundary layer is more readily separated so the separation pressure (effective back pressure) associated with the fuel jet injection process is lower, and by Eq. (5), an increase in penetration may be expected. Further quantification of this

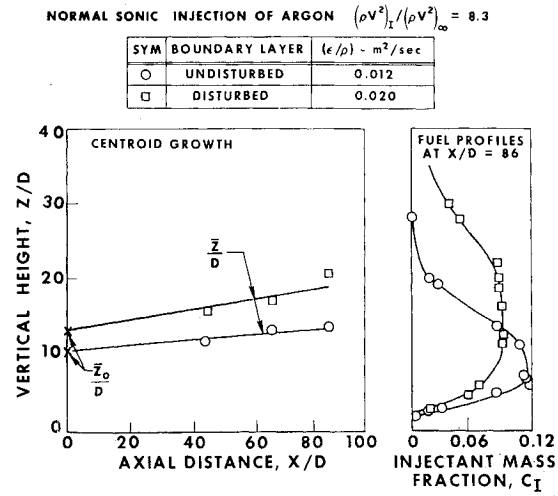

Fig. 12 Effect of approach boundary-layer disturbance on fuel distribution.

process will require more detailed measurements in the three-dimensional injection region.

V. Conclusions

Detailed probe and photographic measurements have been made in a study of the penetration and mixing of (simulated) fuel jets with high-speed airstreams. On the basis of these data, it is concluded that:

1) The centroid of the initial fuel profile as determined from an extrapolation of downstream values, is the appropriate scale length for the two-dimensional region as evidenced by its importance in correlating data.

2) As embodied in the aerodynamic screen concept, a connection exists between the initial jet interaction region and the downstream mixing region.

3. Disturbing the approach flow boundary layer by introducing gas (blowing) at the tunnel wall significantly improves fuel coverage in a combustor because both penetration and the rate of mixing are dramatically increased.

References

[1] Spaid, F. W., "A Study of Secondary Injection of Gases into a Supersonic Flow," Ph.D. thesis, June 1964, California Institute of Technology.

[2] Zukoski, E. E. and Spaid, F. W., "Secondary Injection of Gases into a Supersonic Flow," *AIAA Journal*, Vol. 2, No. 10, Oct. 1964, pp. 1689–1696.

[3] Schetz, J. A. and Billig, F. S., "Penetration of Gaseous Jets Injected into a Supersonic Stream," *Journal of Spacecraft and Rockets*, Vol. 3, No. 11, Nov. 1966, pp. 1658–1665.

[4] Orth, R. C. and Funk, J. A., "An Experimental and Comparative Study of Jet Penetration in Supersonic Flow," *Journal of Spacecraft and Rockets*, Vol. 4, No. 9, Sept. 1967, pp. 1236–1242.

[5] Torrence, M. G., "Concentration Measurements of an Injected Gas in a Supersonic Stream," TN D-3860, Oct. 1966, NASA.

[6] Chrans, L. J. and Collins, D. J., "The Effect of Stagnation Temperature and Molecular Weight Variation of Gaseous Injection into a Supersonic Stream," AIAA Paper 69-1, New York, 1969.

[7] Billig, F. S., Orth, R. C., and Lasky, M., "A Unified Approach to the Problem of Gaseous Jet Penetration into a Supersonic Stream," AIAA Paper 70-93, New York, 1970.

[8] Povinelli, F. P., Povinelli, L. A., and Hersch, M., "Supersonic Jet Penetration (Up to Mach 4) into a Mach 2 Airstream," NASA TM X-52721; also AIAA Paper 70-92, New York, 1970.

[9] Schetz, J. A., Weinraub, R. A., and Mahaffey, R. E., Jr., "Supersonic Transverse Injection into a Supersonic Stream," *AIAA Journal*, Vol. 6, No. 5, May 1968, pp. 933–934.

[10] Schetz, J. A., Hawkins, P. F., and Lehman, H., "Structure of Highly Underexpanded Transverse Jets in a Supersonic Stream," *AIAA Journal*, Vol. 5, No. 5, May 1967, pp. 882–884.

[11] Bogdonoff, S. M. and Kepler, C. E., "Separation of a Supersonic Turbulent Boundary Layer," *Journal of the Aeronautical Sciences*, Vol. 22, No. 6, June 1955, pp. 414–424.

[12] Cohen, L. S., "A New Kinematic Eddy Viscosity Model," Rept. G211709-1, Jan. 1968, United Aircraft Research Labs.

[13] Kilburg, R. F., "A High Response Probe for Measurement of Total Temperature and Total Pressure Profiles Through a Turbulent Boundary Layer with High Heat Transfer in Supersonic Flow," AIAA Paper 68-374, San Francisco, Calif., 1968.

[14] Cohen, L. S., Coulter, L. J., and Chiappetta, L., "Hydrocarbon-Fueled Scramjet," Supplement to Volume VII "Tabulation of Data and Data Reduction Procedures for Fuel Distribution Investigation," TRAFAPL-TR-68-146, March1970, U. S. Air Force.

[15] Crist, S., Sherman, P. M., and Glass, D. R., "Study of the Highly Underexpanded Sonic Jet," *AIAA Journal*, Vol. 4, No. 1, Jan. 1966, pp. 68–71.

[16] Werle, M. J., "A Critical Review of Analytical Method for Estimating Control Forces Produced by Secondary Injection," NDL-TR-68-5, Jan. 1968.